A Comparison of SPH and RANS Models for Simulation of Wave Overtopping

Shahab Yeylaghi* Curran Crawford† Peter Oshkai† Bradley Buckham †

Abstract

Fluid-structure interactions associated with wave overtopping are of significance to many engineering applications. Unsteady wave overtopping loads can lead to significant damage or even failure of the structure. Wave overtopping is a challenging problem to study, since it includes complex phenomenon, such as large deformation of the free surface, air entrainment and turbulence.

Recently, Lagrangian meshless particle methods such as Smoothed Particle Hydrodynamics (SPH) have become an alternative to conventional Eulerian mesh-based methods for studying complex free surface flows. The purpose of the current study is to compare the performance of the explicit incompressible Smoothed Particle Hydrodynamics (SPH) method with experimental data and previous available numerical results for simulation of wave overtopping on a horizontal deck. The free surface profile at different locations and horizontal velocities at the leading edge of the deck, calculated by explicit ISPH method, show good agreement with the experiment and previous numerical study.

Keywords

SPH, Wave overtopping, Irregular wave

1 Introduction

Mesh-less methods were developed to solve problems such as free surface flows with breaking and fragmentation for which conventional CFD methods could not easily be applied [1]. In these methods, a set of discrete particles are scattered over the domain and its boundaries [2]. There is no connectivity (grid) required between particles to solve the PDEs governing the problem [2]. The oldest mesh-less particle method is Smoothed Particle Hydrodynamics (SPH), which was invented in 1970s to study the astrophysical problems including compressible, inviscid flows [3, 4]. Using the unique features of SPH (Lagrangian and mesh-less) make it attractive in different engineering fields, especially hydrodynamics. The main advantage of the relatively computationally expensive SPH over RANS solvers is its ability to capture complex free surface flows [5]. SPH has proved to be a successful numerical method in modeling violent free surface flows [6].

Incompressible fluids in SPH can be modeled either by relating the fluid pressure to particle density by using a stiff equation of state, or by solving Poisson's equation to determine the pressure; the two methods are known as weakly compressible SPH (WCSPH) [7] and incompressible SPH (ISPH) [8], respectively. In the ISPH method, a common approach to solve the Poisson's equation is to solve a set of algebraic equations implicitly, but Hosseini et al. [9] proposed an explicit method to solve the Poisson's equation that doesn't require solving a set of algebraic equations at each time step. Eulerian based CFD methods on other hand do not directly link density variation to pressure. Rather the mass conservation and momentum equations are used to calculate the pressure. WCSPH and ISPH methods are both adept at implicitly including complex free-surfaces, without the need for volume-of-fluid (VOF) or level-set (LS) approaches in RANS. On the other hand, viscosity terms and solid boundary conditions can be more challenging to implement in the SPH methods compared to Eulerian based CFD methods.

The wave overtopping on a horizontal deck is of interest to many engineering applications, such as ship decks, FPSO units [10] and coastal structures [11]. The unsteady loads from the wave overtopping can significantly damage an offshore device [12] and better understanding of wave overtopping loads is needed. More information on wave overtopping can be found in [13, 14].

In this paper, the numerical results of explicit ISPH

*Corresponding author, PhD Candidate, West Coast Wave Initiative, University of Victoria, BC, Canada, shahaby@uvic.ca

†Professor, University of Victoria, BC, Canada

modeling of wave overtopping on a horizontal deck are compared with the experimental data presented earlier by Cox et al. [14]. The results are also compared to volume-of-fluid (VOF) numerical method available in [13].

2 Methodology

In the SPH method, the Lagrangian description of the Navier-Stokes equations are solved for each single fluid particle which represents a finite volume of fluid about a point. The governing equations include the conservation of mass and momentum equations:

$$\frac{1}{\rho}\frac{D\rho}{Dt} + \nabla \cdot \mathbf{u} = 0 \tag{1}$$

$$\frac{D\mathbf{u}}{Dt} = -\frac{1}{\rho}\nabla p + \mathbf{g} + \nu\nabla\mathbf{u}^2 \tag{2}$$

where ρ is the fluid particle density, $\mathbf{u}$ is the particle velocity vector, t is time, p is the particle pressure, $\mathbf{g}$ is the gravitational acceleration vector and ν is the kinematic viscosity. In this method, the domain and its boundaries are represented by discrete volumes of fluid (particles), in which each particle carries material properties, such as velocity, density and viscosity. The flow quantities are interpolated over the predefined neighboring particles using a smoothing function (kernel). The kernel determines the contribution of neighboring particles on the particle of interest's property. The kernel approximation of $A(\mathbf{r})$ in SPH is written as:

$$A(\mathbf{r}) \approx \int_{\Omega} A(\mathbf{x})W(\mathbf{r}-\mathbf{x},h)d\mathbf{x} \tag{3}$$

where $\mathbf{r}$ is the location vector, $A(\mathbf{r})$ is the function of interest at location $\mathbf{r}$, W is smoothing function or kernel defined over domain of interest Ω, and h is the smoothing length which defines the kernel radius (figure 1). The particle approximation of the above integral is obtained by replacing the integral with summation (finite number of particles) as:

$$A_i = \sum_{j=1}^{N} A_j W(\mathbf{r}-\mathbf{r}_j,h)\frac{m_j}{\rho_j} \tag{4}$$

where m_j is the mass of particle j in the neighborhood of particle i and ρ_j is the density of particle j (figure 1). In this study, the fifth order Wendland kernel [15] is used and smoothing length is set to $h = 1.2dr$, where dr is the interparticle distance (figure 1) . Also, the following formulations are adopted for the first order and second order spatial derivatives.

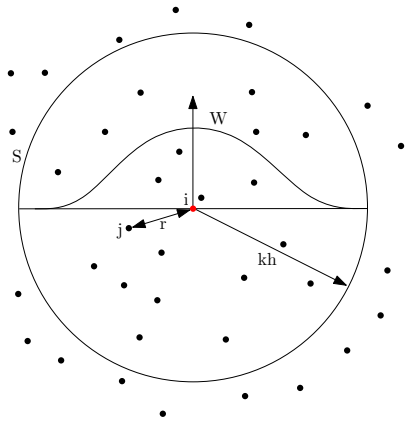

Figure 1: Sketch of the kernel support domain (S) and neighboring particles.

The first order derivative is defined as: [16]:

$$(\nabla A)_i = \rho_i \sum_j m_j \left(\frac{A_j}{\rho_j^2} + \frac{A_i}{\rho_i^2}\right)\nabla_i W_{ij} \tag{5}$$

The second order derivative adopted here is [8, 9]:

$$\nabla \cdot \left(\frac{1}{\rho}\nabla A\right)_i = \sum_{j=1}^{N}\left(\frac{8m_j}{(\rho_i+\rho_j)^2}\frac{A_{ij}\mathbf{r}_{ij}\cdot\nabla_i W_{ij}}{r_{ij}^2+\eta^2}\right) \tag{6}$$

where $\mathbf{r}_{ij} = \mathbf{r}_i - \mathbf{r}_j$, $A_{ij} = A_i - A_j$ and $\nabla_i W_{ij}$ is the gradient of the kernel function at particle i.

The explicit ISPH method [9] is used for this study. This approach is based on the two step projection method that is widely used in Eulerian based methods [8]. In the prediction step, the intermediate velocity is calculated using the viscous and body forces, without pressure force:

$$\mathbf{u}^* = \mathbf{u}(t) + \Delta t(\mathbf{g} + \nu\nabla\mathbf{u}^2) \tag{7}$$

$$\mathbf{r}^* = \mathbf{r}(t) + \Delta t\mathbf{u}^* \tag{8}$$

where $\mathbf{u}^*$ is the intermediate velocity and $\mathbf{r}^*$ is the intermediate position. In the correction step, the incompressibility condition is achieved by correcting the velocity using the pressure force as:

$$\mathbf{u}(t+\Delta t) = \mathbf{u}^* + \Delta t(-\frac{1}{\rho}\nabla p) \tag{9}$$

By taking the divergence of equation 9 and forcing $\nabla\cdot\mathbf{u}(t+\Delta t) = 0$, one can obtain the pressure Poisson's equation which should be solved for pressure at each time step.

$$\nabla \cdot \left(\frac{\nabla p}{\rho}\right) = \left(\frac{\nabla\cdot\mathbf{u}^*}{\Delta t}\right) \tag{10}$$

By using equation (6), the Poisson's equation (10) in particle form can be written as:

$$\sum_{j=1}^{N} 8m_j \left(\frac{1}{\rho_i + \rho_j}\right)^2 \frac{(p_{ij}\mathbf{r}_{ij}) \cdot \nabla_i W_{ij}}{r_{ij}^2 + \eta^2} = \frac{-1}{\Delta t} \sum_{j=1}^{N} V_j \mathbf{u}_{ij}^* \cdot \nabla_i W_{ij} \tag{11}$$

where $p_{ij} = p_i - p_j$, $\mathbf{r}_{ij} = \mathbf{r}_i - \mathbf{r}_j$ and η is a small number. The standard approach to solve the Poisson's equation pressure is an implicit approach. In the implicit approach, at each time step, a set of algebraic equations is solved to find the pressure: i.e. equation (11) will be a system of equations such as, $Ap = b$, where $p_{ij} = p_i^{n+1} - p_j^{n+1}$ (n is the current time step), b is the right-hand side vector and A is the coefficient matrix for each particle.

In this paper, the explicit approach [9] is adapted to solve the Poisson's equation. In the explicit approach, at time $n+1$ the pressure for particle i; p_i^{n+1}, is calculated based on the pressure at neighboring particles at time n; p_j^n (i.e. in equation (11), $p_{ij} = p_i^{n+1} - p_j^n$ and the only unknown will be p_j^{n+1}). By using the explicit approach, solving a set of algebraic equations is not required in each time step; however, a smaller time step must be adopted for accuracy.

3 Results

The important parameters of Cox's experiment [14] are summarized herein-more details can be found in [14]. The experiment includes a piston wavemaker and the still water depth is $0.65m$. The horizontal deck is $0.61m$ long and $0.0115m$ thick. The leading edge of the deck is located at $x = 8m$ from the wavemaker and at $y = 0.0525m$ above still water. The wavemaker signals consists two waves of period $T = 1.0s$ followed by two and a half waves of period $T = 1.5s$ [14]. In order to save computational costs, dimensions of the numerical wave tank are set to $L = 18m$ and $H = 1m$, figure 2. The fluid particle dimensions are set to $dx = 0.0125m$ and $dy = 0.0125m$ which leads to 79932 total particles. Fixed dummy particles are used for the boundary particles as in [9]. A damping zone used in [18] was adopted in this work at the end of the wave tank in order to absorb the wave reflection. The time step is set to $\Delta t = 0.0005s$ for numerical simulations.

The explicit ISPH simulation of the numerical wave tank for the case with deck at $t = 5.7s$ and $t = 10.7s$ are shown in figure 3. The particles are colored for each case by their pressures and velocities, respectively.

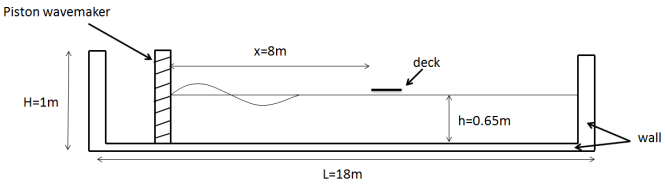

Figure 2: Numerical wave tank.

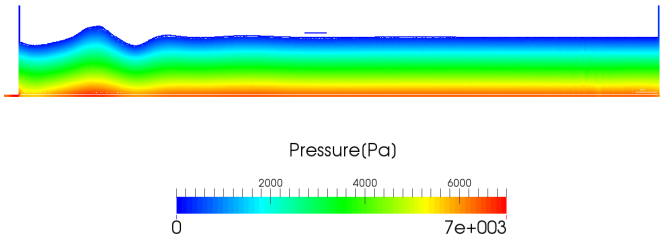

(a) pressure at $t = 5.7s$

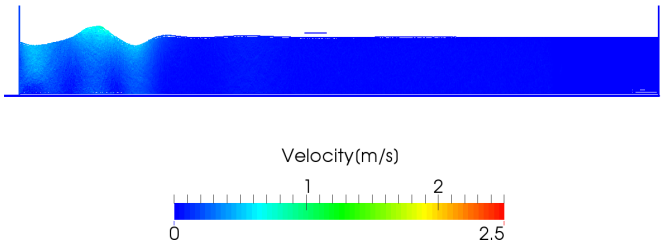

(b) velocity at $t = 5.7s$

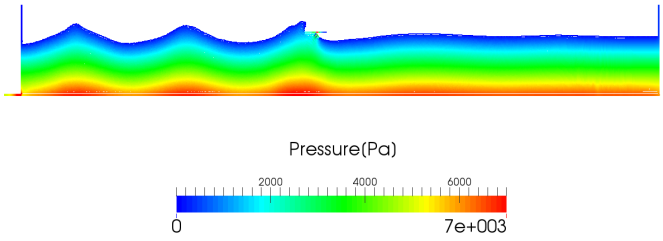

(c) pressure at $t = 10.7s$

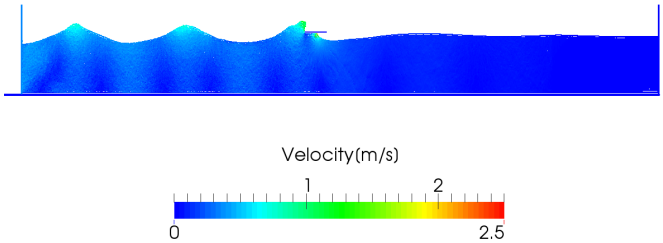

(d) velocity at $t = 10.7s$

Figure 3: Explicit ISPH simulation of numerical wave tank with deck.

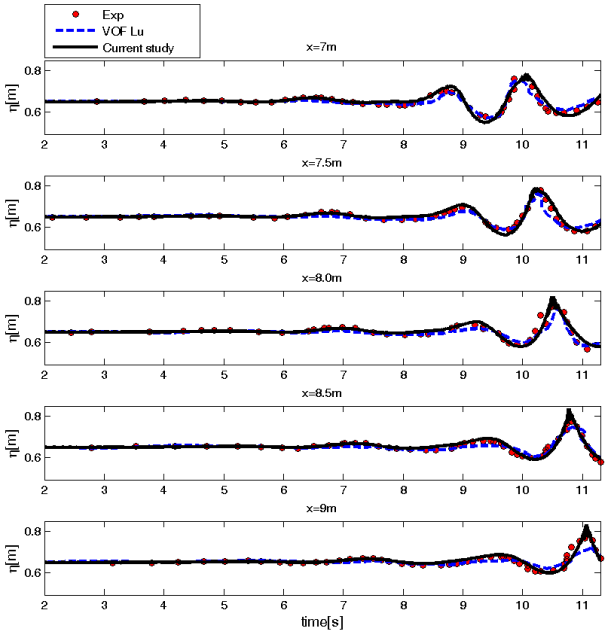

Figure 4: Time history of free surface at different locations obtained from explicit ISPH and plotted vs experimental data [14] and numerical results [13].

The numerical free surface positions at five locations for the case without the deck are calculated based on the explicit ISPH method and shown in figure 4. It is shown that the time histories of the free surface at these locations are in good agreement with experimental measurements [14] and available numerical data [13].

Figure 5a shows the vertical variation of the horizontal velocity in the absence of the deck at four time steps compared with the experimental measurements [14] and previous numerical [13] data. In order to extract the horizontal velocity, the interpolation points were added at the leading edge of the deck, $x = 8m$, and the Wendland kernel [15] was applied in order to obtain the velocities at those points.

Figure 5b shows the vertical variation of the horizontal velocity in the presence of the deck at four time steps compared with previous numerical data in [13] and the experimental measurements in [14]. At $t = 10.22s$ the wave hasn't reached the deck and the horizontal velocity is close to the case without the deck. At $t = 10.58s$ and $t = 10.7s$ the wave has already reached to the deck and the separation in the velocity is clear. At $t = 10.58s$ the maximum velocity occurs above the deck while at $t = 10.7s$ maximum occurs below the deck. The horizontal velocity below the deck at $t = 10.58s$ is smaller than the case without deck while this is vice versa at $t = 10.7s$. At

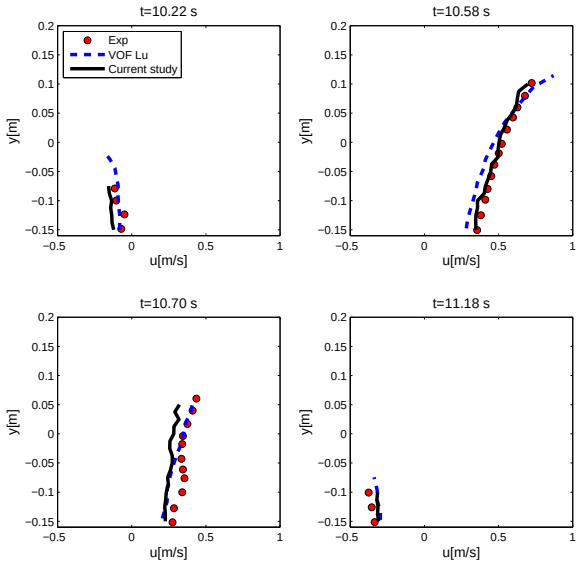

(a) without deck

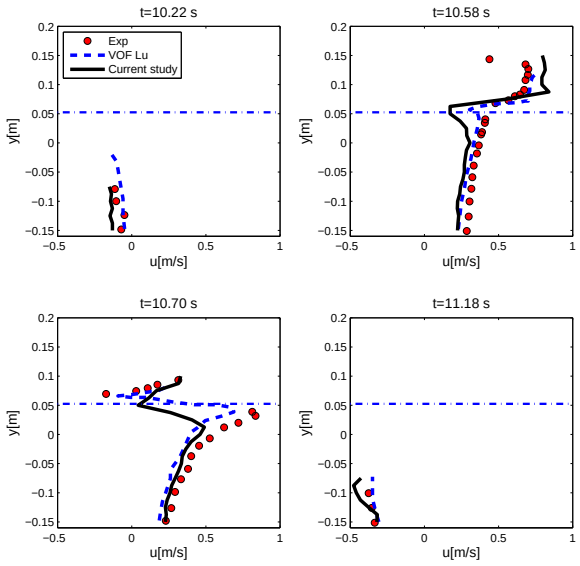

(b) with deck

Figure 5: Vertical variation of the horizontal velocity u (m/s) at leading edge of the deck, $x = 8m$.

$t = 11.18s$ wave has passed the deck and the velocities are close to the values without the deck.

4 Conclusion

An explicit Incompressible Smoothed Particle Hydrodynamics (ISPH) method was applied to model the interaction of two waves with different amplitudes and frequencies and a fixed deck. This method takes advantage of both WCSPH and ISPH methods. It was shown that numerical simulations are in good agreement with experimental data and previous numerical results. This study is part of the future work in simulation of the wave energy converter under wave spectrum.

Acknowledgments

The authors thank the Natural Sciences and Engineering Research Council, Natural Resources Canada, the Pacific Institute for Climate Solutions and the University of Victoria for their financial support.

References

[1] D. Li, *Encyclopedia of microfluidics and nanofluidics*, vol. 1. Springer, 2008. 1

[2] G.-R. Liu and M. Liu, *Smoothed particle hydrodynamics: a meshfree particle method*. World Scientific, 2003. 1

[3] L. B. Lucy, "A numerical approach to the testing of the fission hypothesis," *The astronomical journal*, vol. 82, pp. 1013–1024, 1977. 1

[4] R. A. Gingold and J. J. Monaghan, "Smoothed particle hydrodynamics-theory and application to non-spherical stars," *Monthly notices of the royal astronomical society*, vol. 181, pp. 375–389, 1977. 1

[5] E.-S. Lee, D. Violeau, R. Issa, and S. Ploix, "Application of weakly compressible and truly incompressible sph to 3-d water collapse in waterworks," *Journal of Hydraulic Research*, vol. 48, no. S1, pp. 50–60, 2010. 1

[6] J. Monaghan, "Smoothed particle hydrodynamics and its diverse applications," *Annual Review of Fluid Mechanics*, vol. 44, pp. 323–346, 2012. 1

[7] J. J. Monaghan, "Simulating free surface flows with sph," *Journal of computational physics*, vol. 110, no. 2, pp. 399–406, 1994. 1

[8] S. J. Cummins and M. Rudman, "An sph projection method," *Journal of computational physics*, vol. 152, no. 2, pp. 584–607, 1999. 1, 2

[9] S. Hosseini, M. Manzari, and S. Hannani, "A fully explicit three-step sph algorithm for simulation of non-newtonian fluid flow," *International Journal of Numerical Methods for Heat & Fluid Flow*, vol. 17, no. 7, pp. 715–735, 2007. 1, 2, 3

[10] B. Buchner *et al.*, "The impact of green water on fpso design," in *Offshore technology conference*, Offshore Technology Conference, 1995. 1

[11] C. Franco and L. Franco, "Overtopping formulas for caisson breakwaters with nonbreaking 3d waves," *Journal of Waterway, Port, Coastal, and Ocean Engineering*, vol. 125, no. 2, pp. 98–108, 1999. 1

[12] M. Gómez-Gesteira, D. Cerqueiro, C. Crespo, and R. Dalrymple, "Green water overtopping analyzed with a sph model," *Ocean Engineering*, vol. 32, no. 2, pp. 223–238, 2005. 1

[13] H. Lu, C. Yang, R. Löhner, *et al.*, "Numerical studies of green water impact on fixed and moving bodies," *International Journal of Offshore and Polar Engineering*, vol. 22, no. 2, pp. 123–132, 2012. 1, 2, 4

[14] D. T. Cox and J. A. Ortega, "Laboratory observations of green water overtopping a fixed deck," *Ocean Engineering*, vol. 29, no. 14, pp. 1827 – 1840, 2002. 1, 2, 3, 4

[15] H. Wendland, "Piecewise polynomial, positive definite and compactly supported radial functions of minimal degree," *Advances in computational Mathematics*, vol. 4, no. 1, pp. 389–396, 1995. 2, 4

[16] J. J. Monaghan, "Smoothed particle hydrodynamics," *Annual review of astronomy and astrophysics*, vol. 30, pp. 543–574, 1992. 2

[17] J. P. Morris, P. J. Fox, and Y. Zhu, "Modeling low reynolds number incompressible flows using sph," *Journal of computational physics*, vol. 136, no. 1, pp. 214–226, 1997.

[18] S. Lind, R. Xu, P. Stansby, and B. Rogers, "Incompressible smoothed particle hydrodynamics for free-surface flows: A generalised diffusion-based algorithm for stability and validations for impulsive flows and propagating waves," *Journal of Computational Physics*, vol. 231, no. 4, pp. 1499–1523, 2012. 3